$|p_a| \gg |p_b|$

which, from (6.51), leads to an expression for the length of seal that will theoretically give zero leakage:

$$L_0 = (1/6)[2(\langle p_b\rangle^2 - \langle p_a\rangle^2) - |p_a|^2]c^2/(\mu|U_p||p_a|\sin\phi_a) \qquad (6.52)$$

For machines that have centre ports $\langle p_b\rangle = \langle p_a\rangle$, we have

$$L_0 = -(1/6)|p_a|c^2/(\mu|U_p|\sin\phi_a) \qquad (6.53)$$

where ϕ_a is negative, thus giving a positive value for L_0.

An example is of interest here. The following parameters are taken from a low pressure 1kW free-piston engine (the AT-1000, a prototype of the SPIKE):

$\lvert p_a\rvert = 1.0\times10^5$ Pa	$\phi_a = -28.7°$
$\bar{c} = 14$ µm	$X_p = 15$ mm
$\omega = 377$ rads/s (60 Hz)	$\mu = 20.8\times10^{-6}$ Pa s

for which the ideal seal length is 58 mm, which is a practical number.

Consider, on the other hand a high pressure 2.5 kW free-piston machine:

$\lvert p_a\rvert = 7.6\times10^5$ Pa	$\phi_a = -37.6°$
$\bar{c} = 14$ µm	$X_p = 30$ mm
$\omega = 188.5$ rads/s (30 Hz)	$\mu = 20.8\times10^{-6}$ Pa s.

Here the ideal seal is 346 mm which is likely to be impractical. This, of course, does not mean that a practical machine of these parameters cannot be constructed, but rather that the centre ports would have to be more substantial.

Though it is good practice to design a seal for minimum leakage, it should be expected that the seal will leak somewhat in reality. So, for free-piston machines a centre port is always a necessity. There is a loss associated with the centre port itself. However, in practice the centre port is sized to flow only what is required for stability. Sizing the ports on this basis seems to have a minimal effect on the performance of an engine. As an approximation, the mass flow through the centre port in a half cycle may be taken as being equal to the net mass flow past the seal in the preceding half cycle. This is not strictly true, but it does not seem to be too serious an assumption and it does make the analysis easier.

6.5 Appendix Gap Losses

Frequently it is necessary to use a long piston or displacer to keep the seal remote from the working gas temperature. There is also a clearance gap extending from the hot end to the seal. It is this clearance gap that is responsible for the losses known as appendix gap losses. There are three identifiable irreversibilities that contribute to the appendix gap loss:

(i) shuttle heat transfer
(ii) gas enthalpy transfer
(iii) hysteresis heat transfer.

The shuttle heat transfer is, in effect, a conduction loss down the displacer (or piston) wall, enhanced by the wall's oscillatory motion. Referring to Figure 6.9, it can be seen that when the displacer is at top dead centre, the displacer wall has a lower local temperature than the corresponding cylinder wall temperature at any point along its length. Thus, heat is transferred to the displacer. Conversely, when the displacer is at bottom dead centre, the temperature relationship between the displacer and cylinder is reversed so that heat is transferred from the displacer to the cylinder. Therefore, for the part of the cycle in which the displacer has everywhere a lower temperature than the cylinder, heat moves from the cylinder to the displacer. This heat is carried physically by the displacer and is transferred back to the cylinder at a different axial location where the displacer has everywhere a higher temperature than the cylinder. The displacer motion thus serves to shuttle heat from the hot end to the cold end. Heat transfer to the displacer is by both convection and radiation, the radiation component being typically less than 5% of the overall heat transfer. The shuttle loss mechanism was first identified by Zimmerman and Longsworth in 1970 [ZL70].

The gas enthalpy transfer is simply the net enthalpy transport down the gap by virtue of the working gas motion, pressure and temperature. This loss is sometimes referred to as 'pumping' loss but it is not related to viscous dissipation.

Finally, the hysteresis heat transfer is the net heat transfer from the gas to the cylinder due to temperature gradients set up by the pressure variations in the expansion space. The mechanism is similar to that outlined for the gas spring losses. There is, of course, hysteresis loss associated with the displacer wall, but this is evaluated together with the shuttle loss and is therefore difficult to separate out as an independent mechanism. Typically, the hysteresis loss does not seem to be significant and will be neglected here. However, the hysteresis loss has been obtained in closed-form by this author and is reported in reference [BB81].

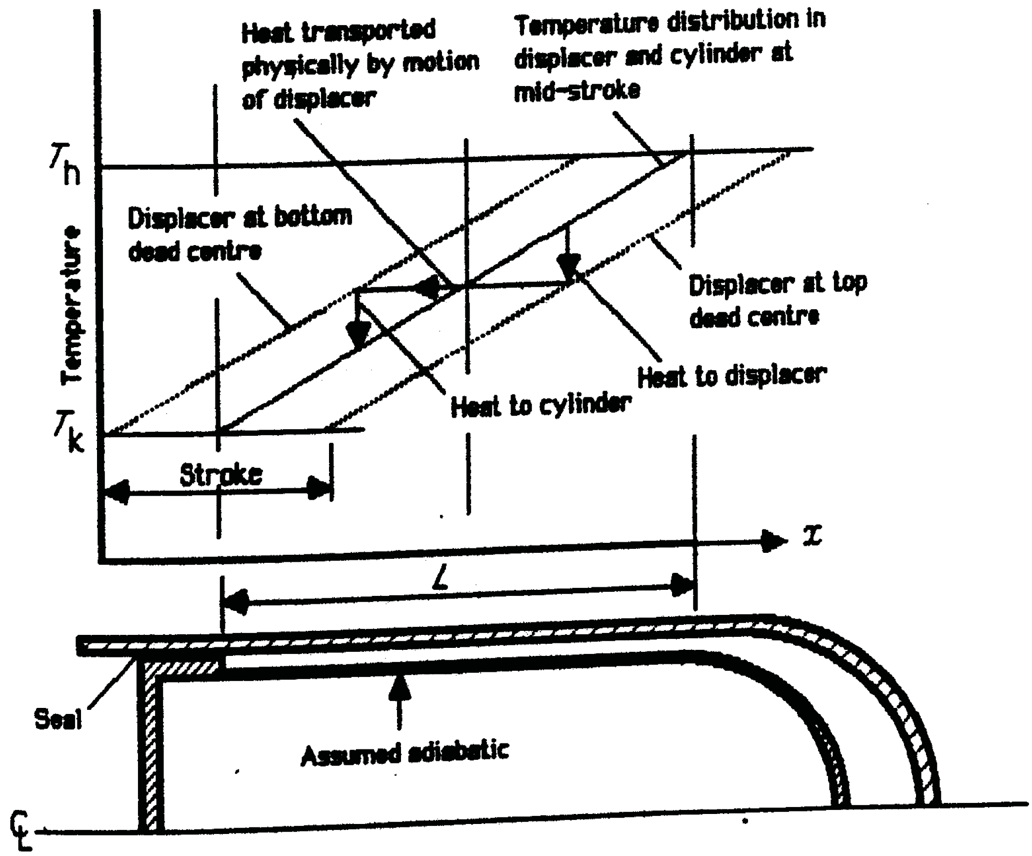

Figure 6.9 Shuttle Loss Mechanism

The following analysis follows that of Rios [Ri71] with some modifications in the treatment of the boundary conditions. However, it should be noted that there is a rigorous but considerably more complicated version of the appendix loss analysis available. This analysis was completed by the author at Mechanical Technology Inc (MTI) for NASA

Lewis under the United States automotive Stirling engine programme [BB81]. For typical engine configurations, the difference between the simplified analysis presented here and the rigorous analysis done at MTI has been between 5% and 10%.

The geometry of the appendix gap and coordinate axis are indicated in Figure 6.10. The origin of the coordinate axis is fixed to the cylinder.

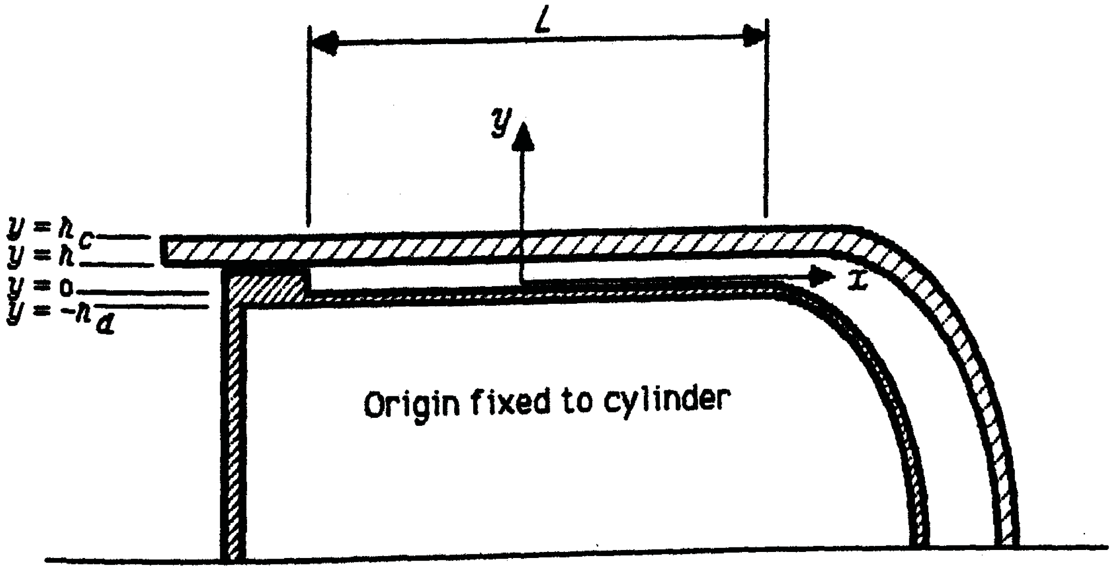

Figure 6.10 Appendix Gap Geometry.

The assumptions made in the analysis are:

1 Static axial conduction is independent of the appendix loss. The thermal effects due to the appendix loss penetrate the wall only as far as the thermal wavelength which is very small compared to the wall thickness.

2 Leakage past the displacer seal is negligible.

3 The gap geometry is treated as two dimensional. This is reasonable since the gap to diameter ratio is small.

4 End effects are negligible.

5 The displacer stroke is short compared with the length of the gap. This assumption allows the temperature distribution to be reasonably approximated by a linear function for the length of stroke.

6 The radial temperature and velocity profiles in the gas are assumed to be linear. In most cases investigated this has been true, since the thermal and viscous boundary layers have been of the same order of size as the gap.

7 Pressure variations and displacer motions may be adequately represented by sinusoids.

8 Transport properties are constant at their mean value.

9 Identical local axial temperature gradients exist in the walls and the gas.

10 The entire assembly is at cyclic steady state.

The prescribed conditions are then:

(a) pressure variation

$$p = \langle p \rangle + |p|\sin(\omega t + \phi) \tag{6.54}$$

(b) displacer motion

$$x_d = X_d \sin\omega t \tag{6.55}$$

Referring again to Equation (6.2), the governing differential energy equation may be simplified by noting that the y direction velocity component is zero and that for the stroke length, the axial temperature is approximately linear. The energy equation thus reduces to

$$\rho c_p(\partial T/\partial t + U\Upsilon) = k\partial^2 T/\partial y^2 + \partial p/\partial t + \Phi \tag{6.56}$$

where $\Upsilon = \mathrm{d}T/\mathrm{d}x$ and is taken as constant at the wall axial temperature gradient.

An order of magnitude study on (6.56) shows that the viscous dissipation term is much smaller than the next smallest term and that the time variation of density is only about 10% of its mean value. The variation of density in the y direction is a little stronger, being about 20% at the cold end and 7% at the hot end. Viscous dissipation may therefore be neglected and density may be assumed locally constant at its mean value without straying too far from reality. The energy equation thus becomes

$$\langle\rho\rangle c_p(\partial T/\partial t + U\Upsilon) = k\partial^2 T/\partial y^2 + \partial p/\partial t\,. \tag{6.57}$$

The velocity profile in the gap is assumed to be instantaneously linear and is therefore given by

$$U = X_d\omega(1 - y/h)e^{j\omega t} \tag{6.58}$$

Putting $\Theta = T - T_s$ where T_s is the local mean temperature and substituting for velocity and pressure, the energy equation becomes

$$\partial\Theta/\partial t - X_d\omega\Upsilon(y/h)e^{j\omega t} = \alpha\partial^2\Theta/\partial y^2 + [|p|e^{j\Phi}/(\langle\rho\rangle c_p) - X_d\Upsilon]\omega e^{j\omega t}. \tag{6.59}$$

By separation of variables, the solution of this is

$$\Theta = [A\exp[(1 + j)\beta y] + B\exp[-(1 + j)\beta y] - jX_d\Upsilon y/h$$
$$- j\{|p|e^{j\Phi}/(\langle\rho\rangle c_p) - X_d\Upsilon\}]e^{j\omega t} \tag{6.60}$$

where $\beta = \sqrt{\omega/(2\alpha)}$ and A and B are constants of integration.

The condition for small gaps is that $h < \sqrt{2\alpha/\omega}$ which is generally true for practical machines. In these cases equation (6.60) may be simplified to

$$\Theta = [A + B\beta y - jX_d\Upsilon y/h - j\{|p|e^{j\Phi}/(\langle\rho\rangle c_p) - X_d\Upsilon\}]e^{j\omega t} \tag{6.61}$$

where A and B are now different constants. This is the final form of the gas temperature field within the appendix gap.

Before the boundary conditions may be applied, the temperature fields for the displacer and cylinder are required. The displacer temperature field is modelled by the temperature field in a solid for a periodic boundary condition. The standard solution is of the form [ED72]

$$T_d^* = T_s^* + \{C\exp[(1 + j)my] + D\exp[-(1 + j)my]\}e^{j\omega t} \tag{6.62}$$

where $m = \sqrt{\omega/(2\alpha_d)}$ and α_d is the thermal diffusivity of the displacer material. This solution is referenced to an axis fixed to the displacer (denoted by the asterisk). We require the solution to be referenced to an axis fixed to the cylinder. Therefore it is necessary to transform the axis by replacing T_s^* with $T_s - \Upsilon X_d \sin\omega t$. Written in terms of Θ, Equation (6.62) becomes

$$\Theta_d = \{C\exp[(1 + j)my] + D\exp[-(1 + j)my] + j\Upsilon X_d\}e^{j\omega t}. \qquad (6.63)$$

The cylinder temperature field is simply

$$\Theta_c = \{E\exp[(1 + j)qy] + F\exp[-(1 + j)qy]\}e^{j\omega t}. \qquad (6.64)$$

where $q = \sqrt{\omega/(2\alpha_c)}$ and α_c is the thermal diffusivity of the cylinder material.

There are six constants in equations (6.61), (6.63) and (6.64): therefore six boundary conditions are required. These are as follows:

1 The heat transfer on the inside wall of the displacer is very much smaller than the heat transfer in the appendix gap. Under this condition, the inner wall may be assumed to be adiabatic:

   Therefore at $y = -h_d$, $d\Theta_d/dy = 0$.

2 The cylinder wall is thick enough so that the outer wall temperature is

constant at T_s. Alternatively, the regenerator, which is often placed in the vicinity of the cylinder wall, would also tend to enforce the outer wall temperature to T_s. Hence

at $y = h_c$, $\Theta_c = 0$.

The four further boundary conditions relate the interface temperatures and conductions.

3 $y = 0$, $\Theta = \Theta_d$

4 $y = 0$, $k d\Theta/dy = k_d d\Theta_d/dy$

5 $y = h$, $\Theta = \Theta_c$

6 $y = h$, $k d\Theta/dy = k_c d\Theta_c/dy$

where k_d and k_c are the thermal conductivities of the displacer and cylinder respectively.

To evaluate the shuttle and enthalpy losses it is only necessary to define the gas temperature field completely. Thus we need only solve for constants A and B In solving for these two constants we shall assume that the displacer and cylinder are made from the same material. This is generally true for engines but not so for cryogenerators or heat pumps, where the displacers are often made from an insulating material.

Defining a thermal conductivity k_s and diffusivity α_s for the solid, we have

$$m = q = \sqrt{\omega/(2\alpha_s)} = w$$

For practical machines $wh_d > 1.5$ and $k/k_s \ll 1$. Using these facts the A and B constants may be simplified a great deal while still retaining good accuracy. Carrying out the above yields:

$$A \approx -|p|/(\langle\rho\rangle c_p)\sin\Phi + j(|p|/(\langle\rho\rangle c_p)\cos\Phi - X_d \Upsilon k/(whk_s)) \tag{6.65}$$

and

$$B \approx 0 \tag{6.66}$$

which are the final forms of the required constants (if greater accuracy is required, eg, for machines where the walls are made of lower conductivity and heat capacity material, then refer to [BB81] where A and B have been calculated to greater accuracy).

The heat transfer to the displacer wall may now be found from the temperature gradient at the wall by differentiating Equation (6.61) with respect to y.

$$\dot{q}_d = k\,d\Theta/dy\Big|_{y=0} \qquad [\mathrm{W/m^2}]$$

$$= k\left[B\beta - jX_d(\Upsilon/h)\right]e^{j\omega t}. \tag{6.67}$$

Noting that B is approximately zero and taking the real part

$$\dot{q}_d = kX_d(\Upsilon/h)\sin\omega t \tag{6.68}$$

which is the heat transfer per unit area to the displacer. As explained previously, the shuttle loss mechanism consists of transporting this heat physically by the motion of the displacer.

Figure 6.11 shows the displacer at two different time instants, x and y are fixed to the cylinder while x^* and y^* are fixed to the displacer.

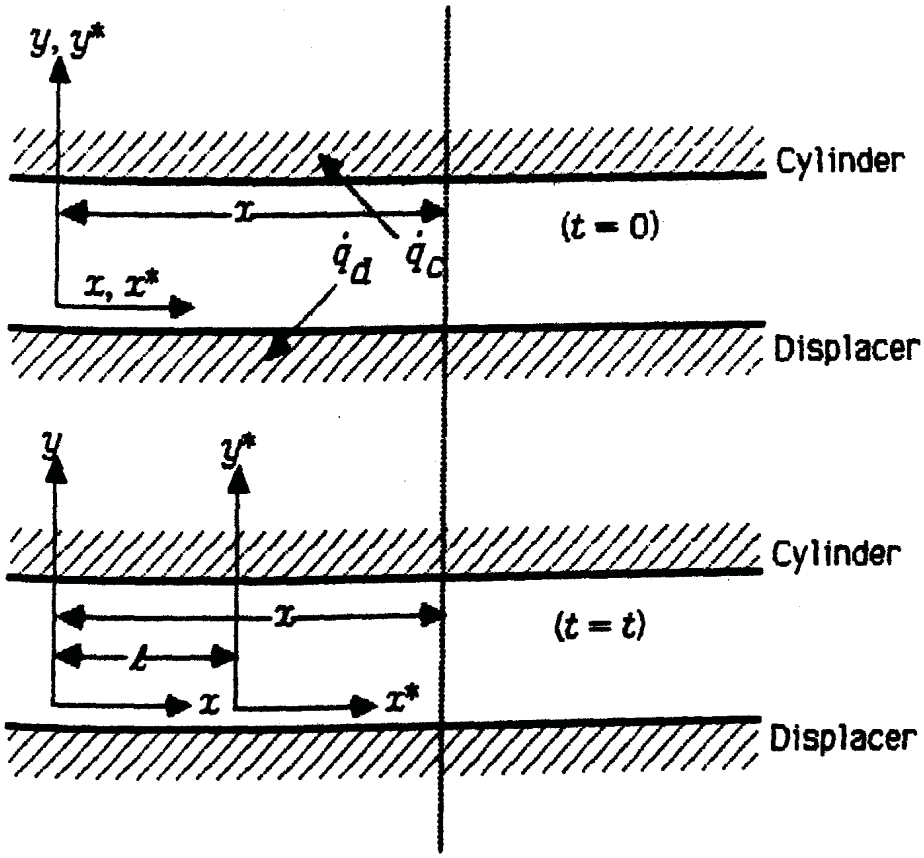

Figure 6.11 Displacer Coordinate Notation.

Defining an internal energy per unit length of the displacer, $\hat{H}_d$:

$$\hat{H}_d = \hat{H}_d(x^*, t) = \int_{A_d} (\rho_d c_d T_d^*) \mathrm{d} A_d \tag{6.69}$$

where ρ_d, c_d and T_d^* are the density, specific heat and local temperature of the displacer. At time t, apply an energy balance to a differential length of the displacer located at x^*:

$$\hat{H}_d(x^*,t) = \hat{H}_d(x^*,0) + \pi D \int_0^t [\dot{q}_d(x^*,t)]dt \tag{6.70}$$

The energy transport across a plane at x and at time t over the instant d t may be expressed as follows:

$$\Delta H_x = (\dot{H}_{x_{gas}})dt + \left[\hat{H}_d(x - \ell, t)\right](d\ell/dt)dt \tag{6.71}$$

where the first term is the gas enthalpy transport and the second is energy transported by the displacer. $d\ell/dt$ is the displacer velocity and x^* has been replaced by $x-\ell$. Substituting Equation (6.70) into Equation (6.71) and integrating over a cycle yields the net energy flow across the x plane:

$$H_x = \oint(\dot{H}_{x_{gas}})dt + \oint \hat{H}_d(x - \ell,0)(d\ell/dt)dt + \pi D \oint\left(\int_0^t \dot{q}_d(x - \ell,t)dt(d\ell/dt)\right)dt \tag{6.72}$$

The second integral is zero since ℓ is periodic and $\hat{H}_d(x - \ell,0)$ is constant with time. The remaining two integrals are the gas enthalpy transfer and the shuttle heat transfer respectively. Noting that

$$\ell = X_d \sin n\omega t$$

and substituting for $\dot{q}_d$ from equation (6.68), the integration for the shuttle heat transfer may be performed, giving

$$H_{sh} = -(\pi^2/\omega) D\, k X_d^2 \Upsilon / h \quad [J] \tag{6.73}$$

or in terms of the mean rate

$$\langle \dot{H}_{sh} \rangle = -(\pi/2) D\, k X_d^2 \Upsilon / h \quad [W] \tag{6.74}$$

which is the final form of the shuttle loss.

The following gas enthalpy transport loss is evaluated differently to that generally found in the literature [Ri69, BB81, UB84]. Rios [Ri69] assumes that the variation of the mass of gas in the appendix volume is in phase with the pressure variations and that the pressure variations are almost in antiphase with the displacer motions. Both these assumptions are not true in engines. Berchowitz [UB84] neglected the change of gas temperature in the gap volume. This assumption could also introduce significant error and can be avoided by taking a slightly different approach.

Gas enthalpy transport is evaluated in the vicinity of the entrance to the cavity. By so doing it is possible to estimate the effect of the expansion space gas entering and leaving the appendix cavity. It is assumed that the temperature of the gas entering the cavity from the expansion space is T_h, and the gas leaving the cavity is at $\bar{T}$, the average temperature across the gap.

The instantaneous enthalpy transport is given by

$$\dot{H}_{L\,gas} = w_a\, c_p\, T \tag{6.75}$$

where $T \leftarrow \bar{T}$ for $w_a \geq 0$ and $T \leftarrow T_h$ for $w_a < 0$

Neglecting leakage, the mass flow into the cavity is simply the negative rate of change of the mass of gas resident in the cavity. The mass of gas in the cavity is given by

$$m_a = p\, V_a / (R\, \bar{T}_L) \tag{6.76}$$

where $\bar{T}_L$ is the mean gas temperature (bulk temperature) averaged in length (L) and width (h) but varies with time.

The average gas temperature across the gap is obtained by integrating the temperature across the gap

$$\bar{T} = 1/h\int_0^h T\,dy \tag{6.77}$$

T is obtained from (6.61) and, since the approximate form of the gas temperature is adequate, the constants A and B may be taken from Equations (6.65) and (6.66). The real part of the temperature is then

$$\bar{T} = T_s - X_d\Upsilon[1/2 - k/(k_s wh)]\sin\omega t \tag{6.78}$$

where the surface temperature (T_s) at the cavity entrance is such that $\bar{T}$ never exceeds T_h, the maximum cycle temperature.

For positive flow, the temperature at the gap entrance may therefore be written

$$\bar{T} = T_h - X_d\Upsilon[1/2 - k/(k_s wh)](1 + \sin\omega t). \tag{6.79}$$

To find the bulk temperature in the cavity, (6.78) is averaged along the cavity length assuming T_s is linear, giving

$$\bar{T}_L = (T_h - T_\ell)/\ln(T_h/T_\ell) - X_d\Upsilon[1/2 - k/(k_s wh)]\sin\omega t \tag{6.80}$$

The volume variations of the cavity are given by

$$V_a = \pi D h(L + X_d\sin\omega t) \tag{6.81}$$

and the pressure variations by equation (6.54).

Substituting (6.54), (6.81) and (6.80) into (6.76):

$$m_a = \langle V_a \rangle \langle p \rangle / (R\bar{T}_L)[1 + r_p \sin(\omega t + \phi)](1 - r_x \sin\omega t)/(1 - r_T \sin\omega t) \tag{6.82}$$

where $r_p = |p| / \langle p \rangle$, $r_x = X_d / L$ and

$r_T = X_d \Upsilon[1/2 - k/(k_s wh)]\ln(T_h / T_\ell)/(T_h - T_\ell)$.

Expanding the denominator by binomial expansion and noting that for practical engines $r_p \ll 1$, $r_x \ll 1$ and $r_T \ll 1$, (6.82) may be written:

$$m_a = \langle V_a \rangle \langle p \rangle / (R\bar{T}_L)[1 + (r_p \cos\phi + r_T - r_x)\sin\omega t + r_p \sin\phi\cos\omega t ... + \mathrm{HOT}] \tag{6.83}$$

where the higher order terms are small.

The mass flow is therefore

$$w_a = -\mathrm{d}m_a/\mathrm{d}t \approx -\omega \langle m_a \rangle [(r_p \cos\phi + r_T - r_x)\cos\omega t - r_p \sin\phi \sin\omega t] \tag{6.84}$$

where $\langle m_a \rangle = \langle V_a \rangle \langle p \rangle / (R\bar{T}_L)$

Substituting for w_a into Equation (6.75) and integrating over a cycle, noting that for positive flow, $\bar{T}$ is given by (6.79) and for negative flow $\bar{T}$

is given by T_h, the net enthalpy transport becomes:

$$\langle \dot{H}_L \rangle_{gas} = -c_p \omega \langle m_a \rangle r X_d \Upsilon [1/2 - k/(k_s w h)](1/\pi - \cos\phi_m/4) \quad [W] \quad (6.85)$$

where $r = [(r_p \cos\phi + r_T - r_x)^2 + (r_p \sin\phi)^2]^{1/2}$

$$\phi_m = \tan^{-1}[(r_p \cos\phi + r_T - r_x)/(r_p \sin\phi)]$$

and noting that here ϕ is defined as the angle at which the pressure leads the displacer (or piston, for alpha machines). ϕ is usually negative (ie, in practice, ϕ is a lagging angle).

In practical engines, the displacer leads the piston by around 60° and the pressure lags the piston by around 20°, the pressure therefore lags the displacer by approximately 80°. If this is assumed in (6.85), then $\phi \approx -80°$ and the cosine terms approach zero while the sine terms approach -1. Furthermore, for typical operating temperatures (T_h = 973K and T_k = 310K), $r_T \approx X_d/(2L)$ and for typical operating parameters, $r_x \approx 0.1$, $r_p \approx 0.1$. With these approximations a useful approximate form of Equation (6.85) may be obtained:

$$\langle \dot{H}_L \rangle_{gas} \approx -\tfrac{1}{2}\gamma/(\gamma - 1)\omega D h \langle p \rangle \ln(T_h/T_l)[[X_d/(2L)]^2 + (|p|/\langle p \rangle)^2]^{1/2} X_d \quad (6.86)$$

where the negative sign indicates a net flow of energy towards the cold end.

To find the net cyclic energy transported down the appendix gap it is necessary to consider a control volume as shown in Figure 6.12. Since the pressure gradient is small, a good ring seal results in negligible leakage loss. If leakage loss is neglected there are still two energy flows required before an energy balance can be made, namely the heat transfer to the cylinder and the pV work on the seal face. The net heat transfer to the cylinder is usually very small compared with the other energy transfers and will therefore not be included here (again, see [BB81]). However, the pV work against the seal face may be significant and should be accounted for.

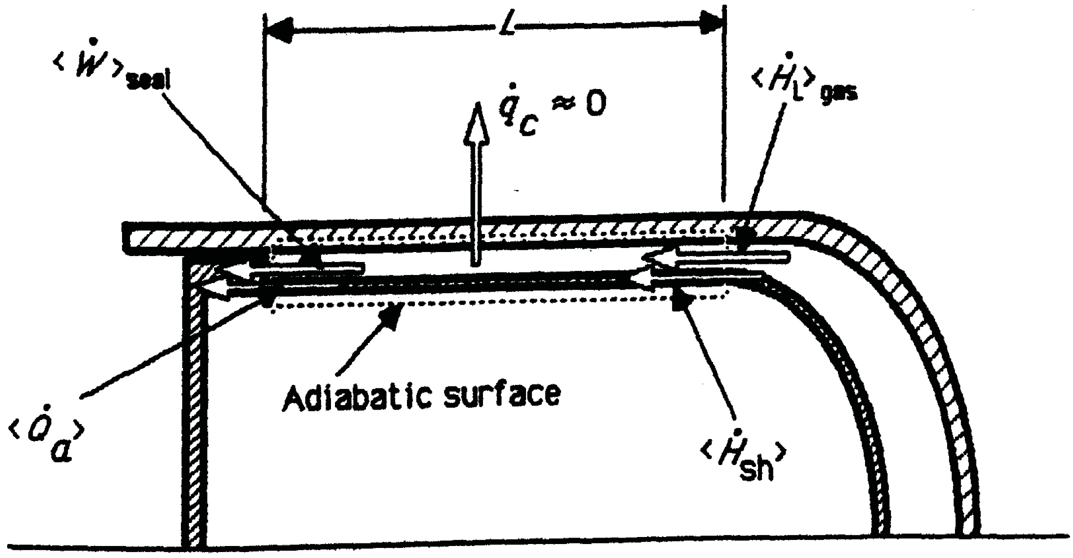

Figure 6.12 Appendix Gap Control Volume.

Neglecting viscous dissipation within the cavity, the pV work is obtained as follows:

$$p\,\mathrm{d}V = -[\langle p \rangle + |p| \sin(\omega t + \phi)]\pi D h X_d \cos\omega t \,\mathrm{d}\omega t.$$

Therefore

$$\langle \dot{W} \rangle_{seal} = -\tfrac{1}{2}\pi D |p| h X_d \omega \sin\phi \ \mathrm{[W]}. \tag{6.87}$$

Since the cyclic change of internal energy is zero, the net energy flow down the displacer is given by

$$\langle \dot{Q}_d \rangle = (-\langle \dot{H}_{sh} \rangle) + (-\langle \dot{H}_L \rangle_{gas}) - \langle \dot{W} \rangle_{seal} \tag{6.88}$$

(positive enthalpy flow towards hot end).

Substituting for each loss and simplifying to the approximate form, the net appendix loss becomes

$$\langle \dot{Q}_d \rangle = (\pi D\, h/2)\Big\{ k(X_d/h)^2 (T_h - T_\ell)/L + \omega \langle p \rangle X_d \Big(\gamma/(\gamma - 1) \ln(T_h/T_\ell) \big[[X_d/(2L)]^2 + (|p|/\langle p \rangle)^2 \big]^{1/2}/\pi - (|p|/\langle p \rangle) \Big) \Big\} \tag{6.89}$$

which is the final form of the appendix loss. A positive value indicates an energy flow towards the cold end.

Figure 6.13 shows the variation of the appendix loss with gap ratio. Also included, for comparison, is the more exact solution in which the gas temperature field is solved for non-linear radial temperature profiles. It can be seen that the linear approximation is good for practical gap sizes.

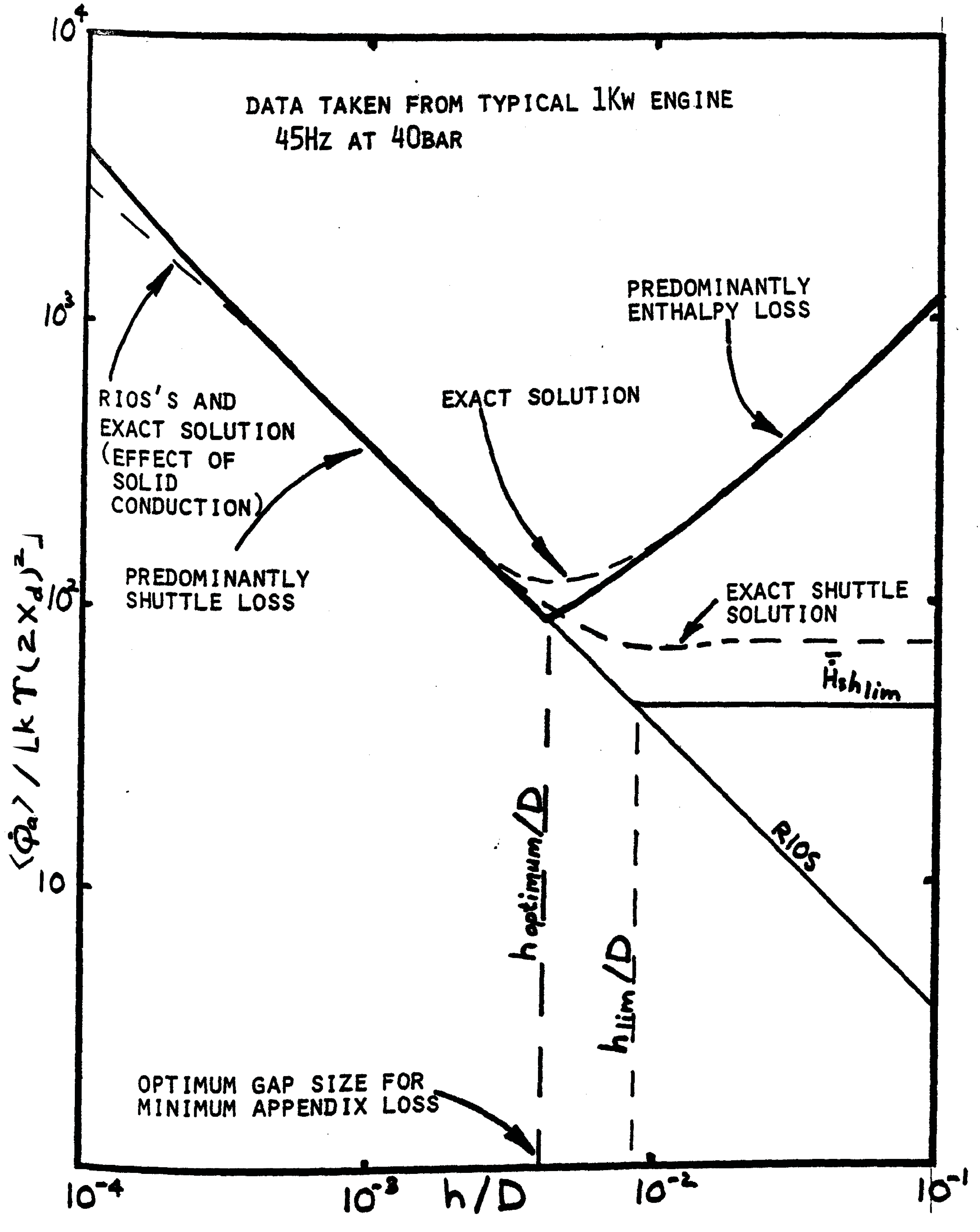

Figure 6.13 Appendix Gap Loss.

The more exact solution [BB81] shows that the shuttle loss reaches a constant value for increasing gap size for gaps larger than twice the gas thermal wavelength. The gas thermal wavelength is given by

$$\lambda = \sqrt{2\bar{\alpha}_h/\omega} \tag{6.90}$$

therefore,

$$h_{lim} = 2\sqrt{2\bar{\alpha}_h/\omega} \tag{6.91}$$

where $\bar{\alpha}_h$ is evaluated at the mean pressure and hot temperature. Substituting into (6.74), the limit shuttle loss would then be

$$\langle \dot{H}_{sh} \rangle_{lim} = -(\pi/4) D k X_d^2 \Upsilon \sqrt{\omega/(2\bar{\alpha}_h)} \tag{6.92}$$

or

$$\langle \dot{H}_{sh} \rangle_{lim} = -(\pi/4) D k X_d^2 \sqrt{\omega/(2\bar{\alpha}_h)}\,(T_h - T_l)/L \tag{6.93}$$

The effect of this limit on shuttle loss is also shown in Figure 6.13.

Since shuttle loss decreases with an increase in gap size (until the limiting value is reached), and the gas enthalpy loss increases with gap size, it is clear that there is an optimum value of h for which the loss is minimised.

Figure 6.14 shows a comparison of the appendix loss calculation with an experiment involving a P40 engine run with different diameter piston domes. This experiment was done at KB United Stirling (Sweden) AB & CO. The appendix gap loss was assumed to account for the increased heat rejected at the cooler. Details of the experiment are unavailable, therefore an error estimation of the experiment is not possible. However, the trend is clearly an increase of rejected heat with reduced piston dome diameter.

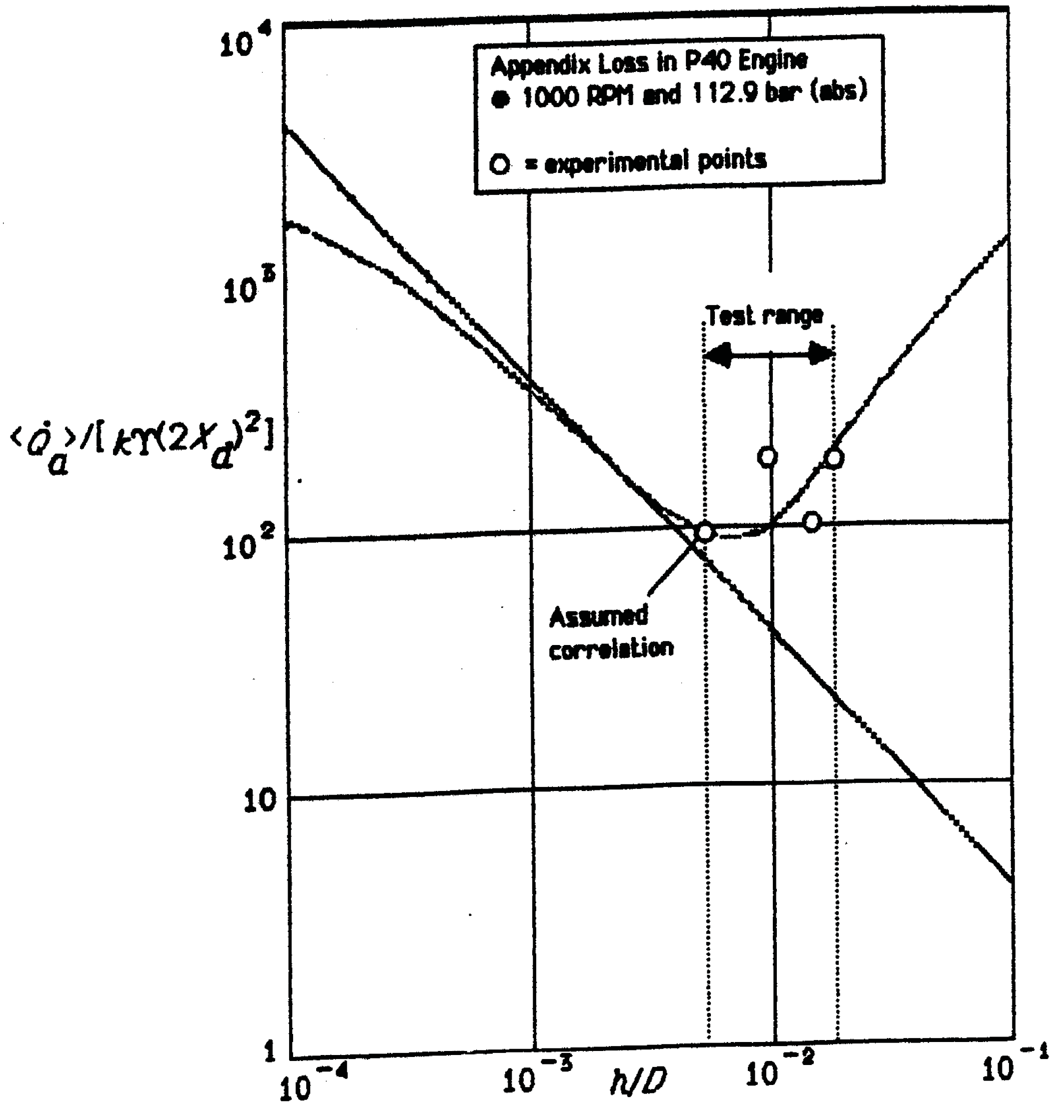

Figure 6.14 Experimental Appendix Gap Loss [BB81]

It now remains to determine how the appendix gap loss alters the performance of the engine cycle. The shuttle component has the effect of simply reducing the resistance of the conduction path down the displacer wall. Therefore, additional heat is transferred to the cold end by conduction, the increase over static conduction being the shuttle loss. Gas enthalpy is more difficult to deal with since for part of the cycle enthalpy is being added to the expansion space and, in the remainder part, enthalpy is extracted from the expansion space. At the same time there is work and heat transfer over the boundaries of the expansion space. Since, in practical engines the expansion space is nearly adiabatic owing to limited heat transfer surface area, it may be assumed that the heat transfer across the boundaries of the expansion space is negligible compared to other energy flows. If a control volume is now drawn to include the entrance to the appendix gap and contain a fixed mass of gas (Figure 6.15), the energy transfers across the boundaries would be the appendix gap enthalpy, pV work at the moving boundaries and enthalpy convected by the working gas itself. The enthalpy convected by the working gas would be small if temperature gradients within the control volume are small compared to gradients along the appendix gap. This condition is likely in practice since the path length of a gas molecule is small compared to the linear dimensions of the expansion space, that is, the gas flow does not penetrate far into the expansion space before returning to the heater. Thus, gas mixing in the expansion space is not isentropic but occurs mainly around the ports to the heater, leaving the core of the expansion space essentially adiabatic. For determining the effects of gas enthalpy transport in the appendix gap, the working gas enthalpy will be neglected. This leaves only pV work on the free boundary and on the displacer dome itself and the gas enthalpy transport into the appendix gap. This situation is identical to the seal model in §6.4 and from first law considerations, implies that the pV work is degraded by an amount equal to the appendix gap enthalpy loss. Thus the gas enthalpy loss degrades the available pV work in the expansion space and appears as additional dissipation to the displacer motion. In a free-piston engine, this effect would be included by the same method as outlined in §5.6 for gas spring hysteresis. It should be noted, however, that the appendix gap enthalpy loss can be handled in a more complete form in numerical simulations as discussed in Appendix D.

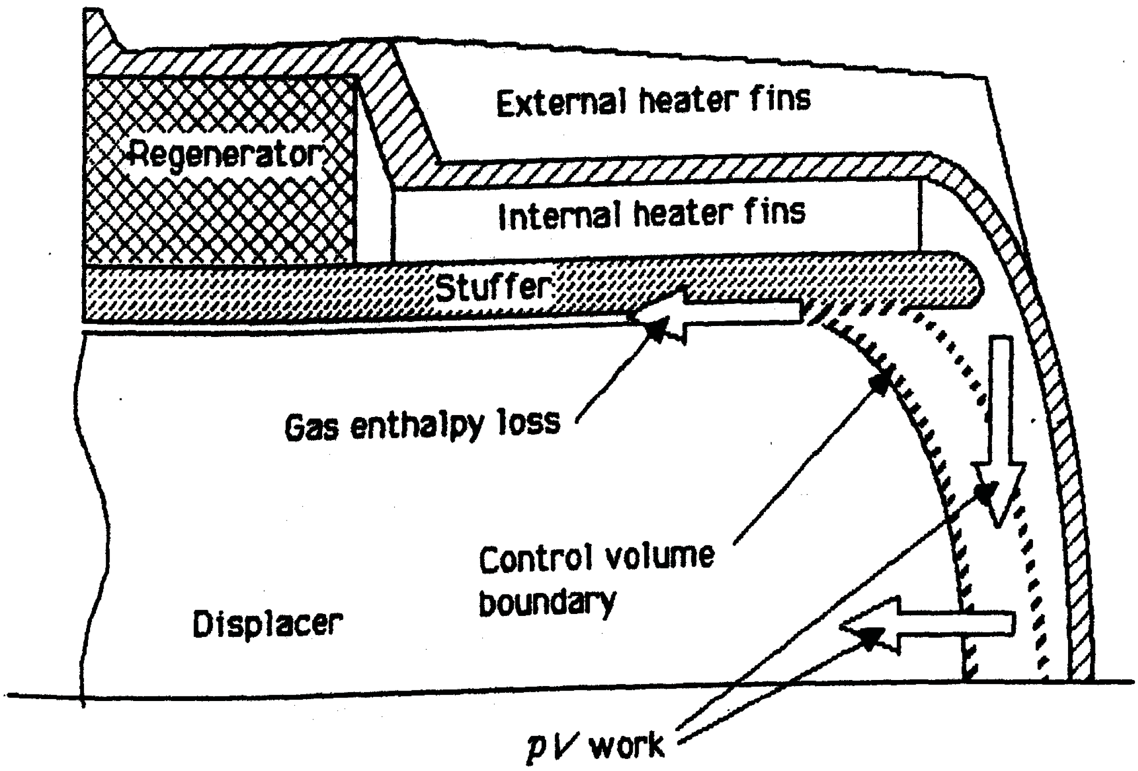

Figure 6.15 Expansion Space Control Volume

6.6 Losses due to Adiabatic Working Spaces

In practical machines the engine speed and cylinder wetted area are such that little significant heat transfer takes place to the gas in the working spaces. Thus the working spaces are usually considered adiabatic. Some workers [LS80, CG84, CR85, Fi60.2] have theoretically demonstrated that if heat transfer is forcibly arranged in the working spaces (eg, by way of extended surfaces), it is possible to actually degrade the efficiency and power of the engine unless the heat transfer is unrealistically high. Benson [BR80] and Martini [MH77] have suggested the use of intermeshing fins (referred to by Benson as *Thermizers* and by Martini as *Isothermalizers*) in order to obtain the necessarily high heat transfer, however, no experimental data seem to be available to indicate their efficacy. Figure 6.15 is taken from Chen, Griffin and West's work [CG84] and indicates the efficiency and power variation versus heat transfer coefficient in the working spaces. By their own account, they could not justify heat transfer coefficients greater than 1000 W/m^2K which, from their figure, would suggest that the adiabatic assumption is reasonable. To get the advantages of the isothermalized engine, their calculations suggest that the heat transfer in the working spaces would have to be increased by nearly four orders of magnitude. If the gas in the working spaces is not highly agitated then the hysteresis heat transfer should be an approximate indication of the degree of heat transfer likely in the working spaces. As will be shown in the next section, for the engines analysed here, the working space hysteresis heat transfer does not seem to be significant. For this work, therefore, adiabatic working spaces are assumed to be representative of practical machines. No attempt has been made to separate out the loss due to adiabatic working spaces as compared to the isothermal assumption. The effects of the adiabatic working spaces are accounted for in the development of the basic analysis of the cycle. This cycle has been referred to as the pseudo Stirling cycle [RU77] or the ideal adiabatic Stirling cycle [UB84]. A semi closed-form analysis of it is described in detail in Appendix C.

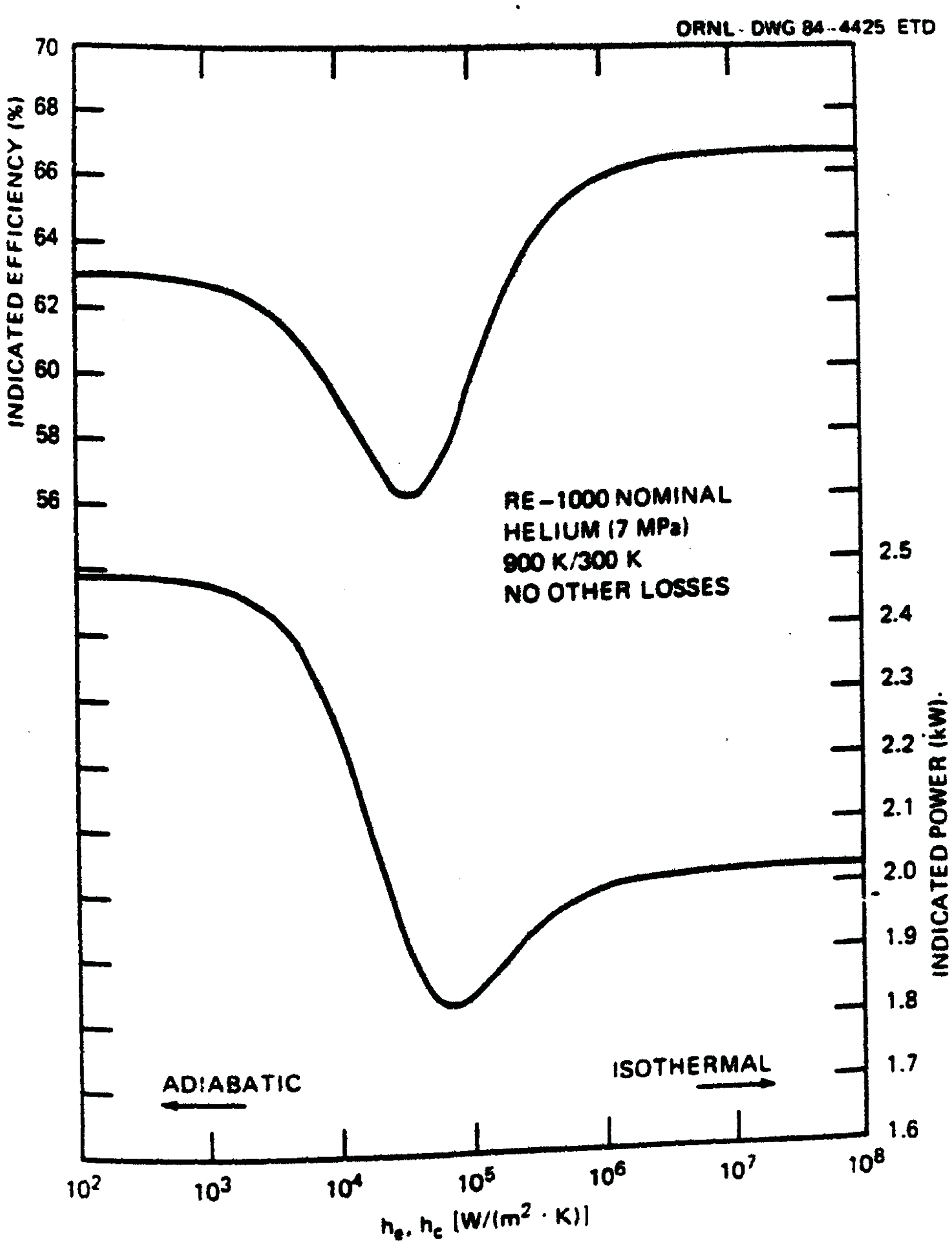

Figure 6.16 Effect on Performance due to Heat Transfer in the Working Spaces [CG84]

Chen *et al* have compared the reduction in efficiency of the ideal adiabatic cycle to the isothermal cycle for increasing compression ratio. Figure 6.17 is taken from Chen *et al*'s work [CG84] and clearly indicates the drop off of efficiency with increased compression ratio. It is interesting to note that though this comparison was obtained by second order methods, the trends are very similar to the simple cycle analysis done by Rallis (discussed in §2.2 and §2.3).

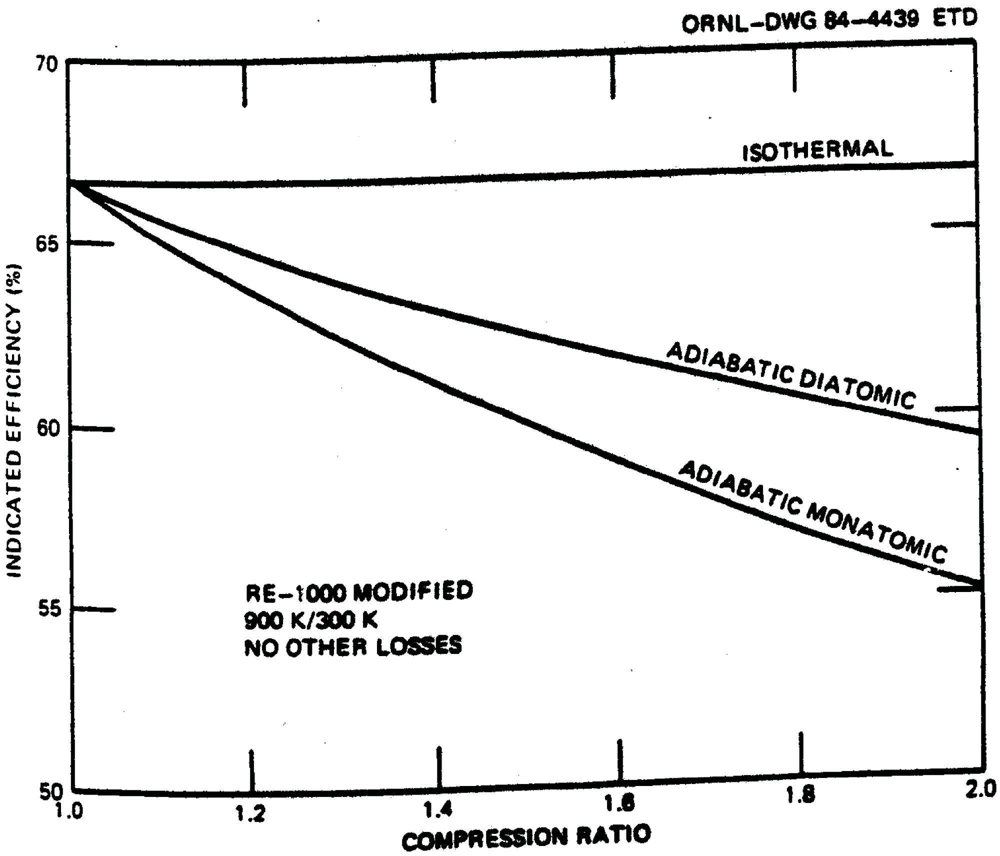

Figure 6.17 Reduction of Efficiency with Increasing Compression Ratio [CG84]

6.7 Mechanical Losses

In the case of crank driven machines, mechanical losses simply reduce the output power by an amount equal to the work dissipated against mechanical friction. Typically this would include seal friction and bearing friction. For free-piston machines the situation is a little different in that added mechanical friction on the displacer results in not only the obvious dissipated power, but also in a reduction of the displacer amplitude which then reduces the available power even more. There is also a secondary effect on the displacer/piston phase angle. If care is not taken, it is possible for a small mechanical loss to greatly reduce the output power and make the engine difficult or impossible to start (see S5.4, Equation (5.64)). In order, therefore, to obtain a meaningful analysis of free-piston engines, it is necessary to evaluate the mechanical losses. Since in a crank machine the mechanism losses do not have a fundamental effect on the cycle they will not be included in this work.

The major mechanical loss in free-piston engines is the seal or ring friction. Figure 6.18 shows a ring seal in a groove of a reciprocating element with a differential pressure across it.

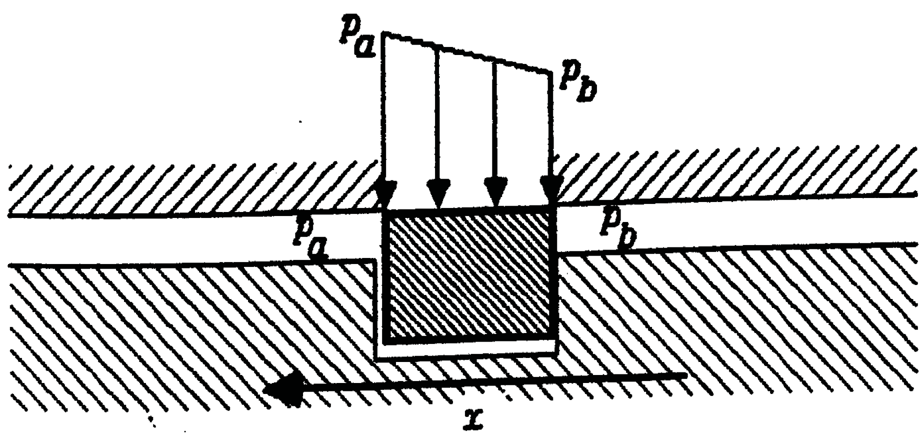

Figure 6.18 Ring Seal

Assuming a linear pressure profile across the face of the seal, the work done by the force exerted on the moving surface by the seal is given by

$$W_s = \oint F\,dx = \oint \mu\,(\Delta p/2)\,A_s\,dx$$
$$= 0.5\mu A_s \oint \Delta p (dx/d\theta) d\theta \qquad (6.94)$$

where μ is the coefficient of friction and A_s is the seal area in contact with the sliding surface.

For arbitrary sinusoidal pressure variations on either side of the seal (as in §6.4) and motion given by

$x = X\sin\theta$,

the seal work becomes

$$W_s = 0.5\mu A_s X \oint \left| \left[|p_a|\sin(\theta + \phi_a) - |p_b|\sin(\theta + \phi_b) \right] \cos\theta \right| d\theta$$
$$= \mu A_s X \left[\left| (|p_a|\cos\phi_a - |p_b|\cos\phi_b) \right| + (\pi/2) \left| (|p_a|\sin\phi_a - |p_b|\sin\phi_b) \right| \right] \qquad (6.95)$$

Sometimes the seals are spring loaded which results in a constant friction force over and above the pressure activated force. In this case there is additional seal work as follows

$$W_{sc} = \oint |F_{sc}\,(dx/d\theta)|\,d\theta$$
$$= 4F_{sc}X \qquad (6.96)$$

where F_{sc} is the constant friction force which would be determined empirically.